LYSET facilitates integration of both the N- and C-terminal transmembrane helices/cytoplasmic domains of GlcNAc-1-phosphotransferase

Baraj Doray[a,*], Benjamin C. Jennings[a], Xi Yang[b,†], Lin Liu[c], Varsha Venkatarangan[b], Stuart Kornfeld[a], and Ming Li[b,*]

[a]Department of Internal Medicine, Washington University School of Medicine, St. Louis, MO 63110;
[b]Department of Molecular, Cellular, and Developmental Biology, University of Michigan, Ann Arbor, MI 48109;
[c]M6P Therapeutics, St. Louis, MO 63108

ABSTRACT LYSET is a recently identified Golgi transmembrane (TM) protein, and inactivating mutations in the *LYSET* gene phenocopy mucolipidosis II (MLII), the lysosomal storage disease caused by loss of function of GlcNAc-1-phosphotransferase $\alpha\beta$ (GNPT$\alpha\beta$), which tags lysosomal hydrolases with the mannose 6-phosphate (M6P) tag for delivery to lysosomes. It is conceivable that LYSET facilitates integration of both hydrophilic TM helices (TMHs) of GNPT$\alpha\beta$ and retain the latter in the Golgi, although this has only been directly demonstrated for the N-terminal TMH wherein a membrane-stabilized GNPT$\alpha\beta$ variant restores lysosomal function in cells lacking LYSET. Here we show that the C-terminal TMH of GNPT$\alpha\beta$ also contributes to LYSET-mediated Golgi retention. In addition, disease-causing patient mutations in the N-terminal TMH of GNPT$\alpha\beta$, which increase the hydrophilicity of the helix, are partly rescued by overexpression of LYSET. Finally, we show that a membrane-stabilized GNPT$\alpha\beta$ variant, despite overcoming the requirement for LYSET, still requires COPI-mediated recycling via the N-terminal cytosolic domain (CD) for GNPT$\alpha\beta$ retention and function in the Golgi.

⚠ Challenge

✕ Cross-Validation

💡 New Hypothesis

SIGNIFICANCE STATEMENT

- Inactivation of the *LYSET* gene phenocopies mucolipidosis II, caused by loss of GNPT$\alpha\beta$ function. A complete picture of how LYSET works with GNPT$\alpha\beta$ is still lacking.
- The authors show that both the N- and C-terminal TMHs/CDs of GNPT$\alpha\beta$ participate in LYSET-mediated regulation of function. Also, patient mutations in the N-terminal TMH of GNPT$\alpha\beta$ that increase the hydrophilicity of the helix can be partly rescued by overexpression of LYSET. Finally, LYSET alone is insufficient for Golgi retention of GNPT$\alpha\beta$ without COPI recycling.
- These findings provide additional insight into how LYSET functions as a Golgi tether for GNPT$\alpha\beta$.

INTRODUCTION

In vertebrates, the proper targeting of newly synthesized lysosomal hydrolases via the mannose 6-phosphate (M6P) pathway to the lysosome is crucial for the degradation of intracellular and endocytosed materials (Kornfeld, 1986). A number of diseases collectively known as lysosomal storage disorders (LSDs) arise as a result of defects in this pathway (Kollmann et al., 2010). Key among these is the severe LSD termed mucolipidosis II (MLII), and a milder version of the disease, mucolipidosis III $\alpha\beta$ (MLIII $\alpha\beta$). Both diseases result from mutations in the *GNPTAB* gene that encodes the α and β subunits of the enzyme GlcNAc-1-phosphotransferase (GNPT$\alpha\beta$) (Kudo et al., 2005; Paik et al., 2005; Tiede et al., 2005; Kudo et al., 2006).

GNPT$\alpha\beta$ is initially synthesized as an inactive precursor type-III polypeptide chain in the endoplasmic reticulum (ER). Upon arrival at the *cis*-Golgi, the precursor molecule undergoes proteolytic cleavage between residues 928 and 929 mediated by Site-1 protease (S1P) to give rise to the individual α and β subunits, a step that is essential for its phosphotransferase (ptase) catalytic activity (Marschner et al., 2011). Activated GNPT$\alpha\beta$ performs the initial and most crucial step in the generation of the M6P recognition marker on newly synthesized acid hydrolases by transferring GlcNAc 1-phosphate from UDP-GlcNAc to specific mannose residues on the high mannose glycan chains of lysosomal enzymes. Following this step, uncovering enzyme (N-Acetylglucosamine-1-phosphodiester α-N-acetylglucosaminidase) removes GlcNAc to form the M6P monoester on the glycan chain. At the *trans*-Golgi network (TGN), the M6P moiety serves as a high-affinity ligand for binding of the hydrolases to M6P receptors, which are packaged into clathrin-coated vesicles for onward transport to the endolysosomal system (Ghosh et al., 2003). GNPT$\alpha\beta$ steady-state localization in the *cis*-Golgi is imperative to ensure the fidelity of this process, as illustrated by disease-causing patient mutations in its N-terminal cytoplasmic domain (CD) which lead to the mislocalization and degradation of GNPT$\alpha\beta$ in lysosomes (van Meel et al., 2014).

TMEM251/GCAF/LYSET (LYSET) is a Golgi transmembrane (TM) protein recently shown to be critical for lysosome biogenesis. In cells lacking LYSET, GNPT$\alpha\beta$ activity is lost, and acid hydrolases are secreted rather than sorted to the lysosome, resulting in an MLII disease phenotype (Pechincha et al., 2022; Richards et al., 2022; Zhang et al., 2022). Moreover, patients with loss-of-function mutations in the *LYSET* gene present symptoms similar to those seen in MLII and die in childhood or early adulthood (Ain et al., 2021). These findings underscore the critical role of LYSET in the M6P pathway. Additionally, our more recent data indicate that the LYSET-mediated Golgi localization of GNPT$\alpha\beta$ is achieved by vesicular recycling of both proteins involving COPI, Golph3, and retromer (Yang et al., 2024).

The N- and C-terminal TM helices (TMHs) of GNPT$\alpha\beta$ display unusually strong hydrophilic properties (Braulke et al., 2024). Amino acid substitutions within the N-terminal TMH, whereby two hydrophilic amino acids were substituted for hydrophobic residues (Q36L/E39L), restored GNPT$\alpha\beta$ function in cells lacking LYSET (Pechincha et al., 2022). In this study, we investigated whether the C-terminal TMH of GNPT$\alpha\beta$ also contributes to membrane stabilization and Golgi retention mediated by LYSET. Further, we analyzed the effect of disease-causing patient mutations within the N-terminal TMH of GNPT$\alpha\beta$ on the amphipathicity of the helix and asked whether overexpression of LYSET can rescue these mutations. Finally, we addressed the broader function of membrane stabilization versus vesicular recycling and the relative contribution of each to the steady-state localization of GNPT$\alpha\beta$ in the Golgi.

RESULTS AND DISCUSSION

GNPT$\alpha\beta$ Q36L/E39L activity is reduced in *LYSET*$^{-/-}$ HEK293T cells

The first clue that the TMHs of GNPT$\alpha\beta$ may play a role in Golgi retention came from our earlier study where we analyzed the consequence of disease-causing patient mutations within the N-terminal TMH that resulted in the mutant proteins being missorted to the lysosome and be degraded (Lee et al., 2020). This led us to propose that these mutations either impaired the proper association of the TMH with the lipids of the Golgi membrane or affected the association of GNPT$\alpha\beta$ with another protein which is necessary for proper Golgi localization. Following the discovery of LYSET, it was reported that a membrane-stabilized Q36L/E39L variant could restore GNPT$\alpha\beta$ localization to the Golgi and ptase-dependent cellular functions in cells lacking LYSET (Pechincha et al., 2022). Although there was no discernable variation of Q36L/E39L expression between wild-type (wt) and LYSET knockout human pancreatic carcinoma (MIA PaCa-2) cells, immunoblot analysis revealed a significant difference in the protein level of this variant between parental wt and *LYSET*$^{-/-}$ HEK 293T cells (Pechincha et al., 2022). Hence, we first directly assayed the ptase activity of GNPT$\alpha\beta$ Q36L/E39L expressed exogenously in wt cells to compare it with *LYSET*$^{-/-}$ 293T cells to quantify the difference. Whole-cell lysates (WCL) prepared from transfected cells were used to measure the transfer of radiolabeled GlcNAc-1P from the nucleotide sugar donor UDP-GlcNAc to the synthetic acceptor α-MM. The level of endogenous GNPT$\alpha\beta$ in cells is extremely low and its ptase activity is below the detection limit in our assay (van Meel et al., 2016). Using this assay, we have previously determined that under conditions of low-level exogenous expression (400 ng of transfected DNA), the ptase activity of wt GNPT$\alpha\beta$ is dramatically decreased ($\sim$15-fold) in *LYSET*$^{-/-}$ 293T cells relative to parental cells. For GNPT$\alpha\beta$ Q36L/E39L, a 2.5-fold decrease in activity was observed in *LYSET*$^{-/-}$ cells (Figure 1A, compare lanes 3 and 4), a significantly smaller fold change than with wt GNPT$\alpha\beta$. Nevertheless, the decreased activity of GNPT$\alpha\beta$ Q36L/E39L in the absence of LYSET indicated the latter can still regulate this gain-of-function variant. Consistent with this finding, increasing amounts of LYSET

Abbreviations used: α-MM, Methyl α-D-mannopyranoside; CD, cytosolic domain; ER, endoplasmic reticulum; GNPT$\alpha\beta$, GlcNAc-1-phosphotransferase $\alpha\beta$; LSDs, Lysosomal Storage Disorders; M6P, mannose 6-phosphate; ML II, mucolipidosis II; ptase, phosphotransferase; TGN, trans-Golgi network; TM, transmembrane; TMHs, transmembrane helices.

	1	2	3	4
Parental 293T cells	+	-	+	-
LYSET$^{-/-}$ 293T cells	-	+	-	+
Vector (ng)	2000	2000	1600	1600
GNPTαβ Q36L/E39L (ng)	0	0	400	400

	1	2	3	4	5	6
Vector (ng)	2000	1600	1100	600	100	500
GNPTαβ Q36L/E39L (ng)	0	400	400	400	400	0
LYSET (ng)	0	0	500	1000	1500	1500

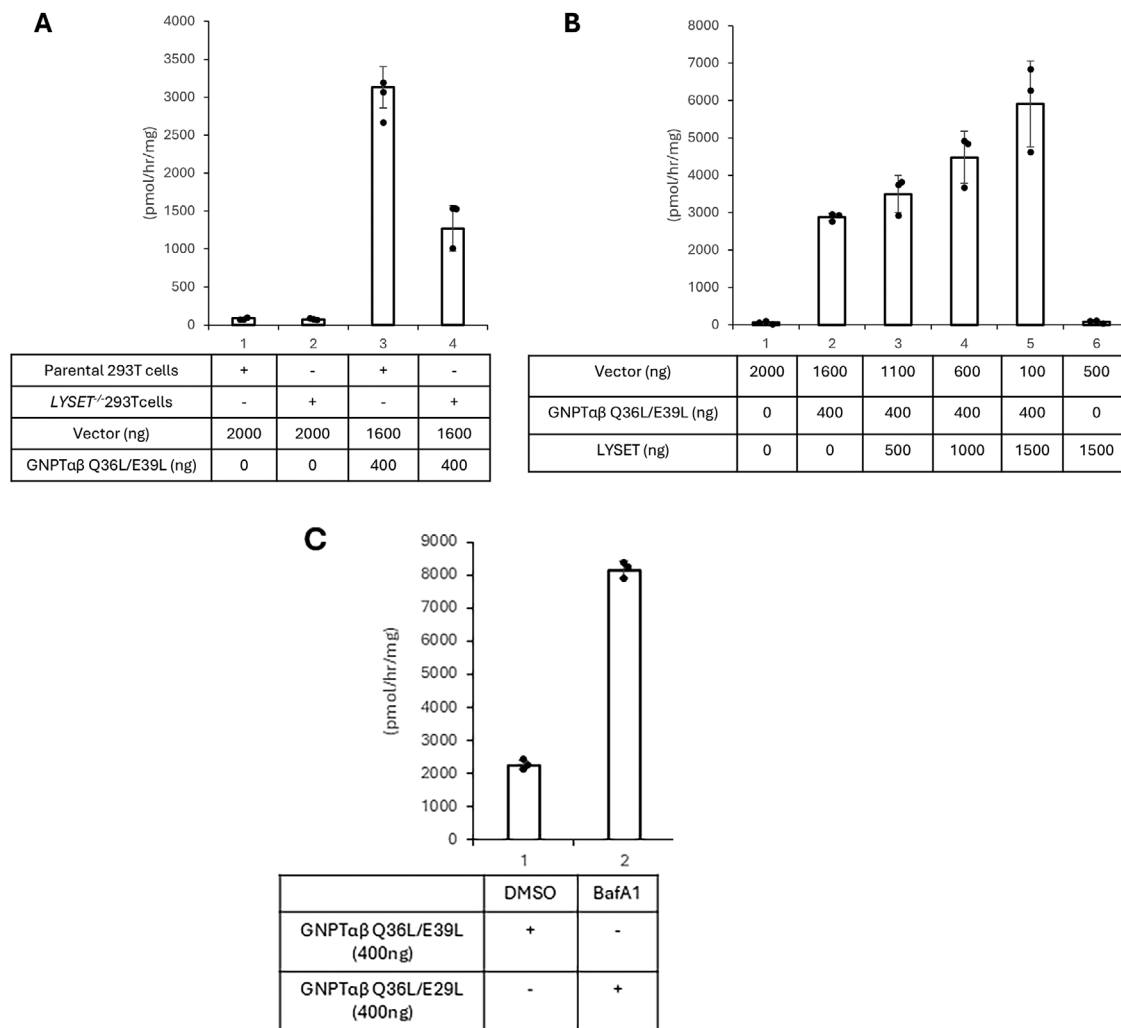|	DMSO	BafA1
GNPTαβ Q36L/E39L (400ng)	+	-
GNPTαβ Q36L/E29L (400ng)	-	+

FIGURE 1: Endogenous LYSET elevates GNPT$\alpha\beta$ Q36L/E39L ptase activity, while exogenous expression of LYSET increases activity in a dose-dependent manner in *LYSET*$^{-/-}$ 293T cells. (A) Comparison of GNPT$\alpha\beta$ Q36L/E39L ptase activity between transfected wt and *LYSET*$^{-/-}$ 293T cells. A total of 400 ng of GNPT$\alpha\beta$ Q36L/E39L plasmid cDNA was combined with 1600 ng of vector DNA (pcDNA3.1) for transfection into each well of a 6-well plate. ptase activity is calculated as described in *Materials and Methods*. (B) ptase activity of transfected *LYSET*$^{-/-}$ 293T cells expressing GNPT$\alpha\beta$ Q36L/E39L with increasing amount of coexpressed LYSET. (C) *LYSET*$^{-/-}$ 293T cells transfected to express GNPT$\alpha\beta$ Q36L/E39L were treated 32 h posttransfection with either DMSO or 100 nM BafA1 for 16 h before cells were collected and processed for ptase assay. All activity data are mean ± SD for three independent transfections.

cDNA cotransfected with a constant amount (400 ng) of GNPT$\alpha\beta$ Q36L/E39L cDNA increased the ptase activity of this variant in a dose-dependent manner with a 2.1-fold elevation observed at maximal LYSET expression (Figure 1B), in agreement with the increased expression of GNPT$\alpha\beta$ Q36L/E39L in MIA PaCa-2 cells when LYSET was overexpressed (Pechincha *et al.*, 2022). To verify that a population of GNPT$\alpha\beta$ Q36L/E39L still exits the Golgi and is trafficked to the lysosome to be degraded with some fraction possibly secreted to the outside of the cell (van Meel *et al.*, 2014), *LYSET*$^{-/-}$ transfected cells were treated with 0.1 μM Bafilomycin A1 (BafA1) for 16 h. BafA1 is known to prevent Golgi exit and degradation in the lysosome (Tawfeek and Abou-Samra 2004; van Meel *et al.* 2014). In addition, we have shown that BafA1 stabilizes wt GNPT$\alpha\beta$ by preventing its exit from the Golgi rather than by inhibiting lysosomal degradation (Yang *et al.*, 2024). Under these conditions, a 3.6-fold increase in activity of GNPT$\alpha\beta$ Q36L/E39L was observed (Figure 1C). Taken together, these results show that despite

being membrane stabilized by the two amino acid changes, a significant portion of GNPT$\alpha\beta$ Q36L/E39L is still exiting the Golgi in the absence of LYSET and this effect can be prevented by exogenous expression of LYSET.

Golgi retention mediated by LYSET is lost with GNPT$\alpha\beta$ lacking both TMHs

We then asked whether this increased stabilization and Golgi retention of GNPT$\alpha\beta$ Q36L/E39L is occurring through the C-terminal TMH. Before addressing this issue, we first determined the consequence of deleting both TMHs and comparing wt GNPT$\alpha\beta$ expression with this soluble form in *LYSET*$^{-/-}$ 293T cells. To accomplish this, it was necessary to switch the S1P cleavage site with a furin cleavage site for efficient cleavage and engineer in the Igκ light chain signal peptide sequence at the N-terminus to generate a soluble form of GNPT$\alpha\beta$ that is catalytically active (Kudo and Canfield, 2006). Activity assays performed using WCL revealed greater
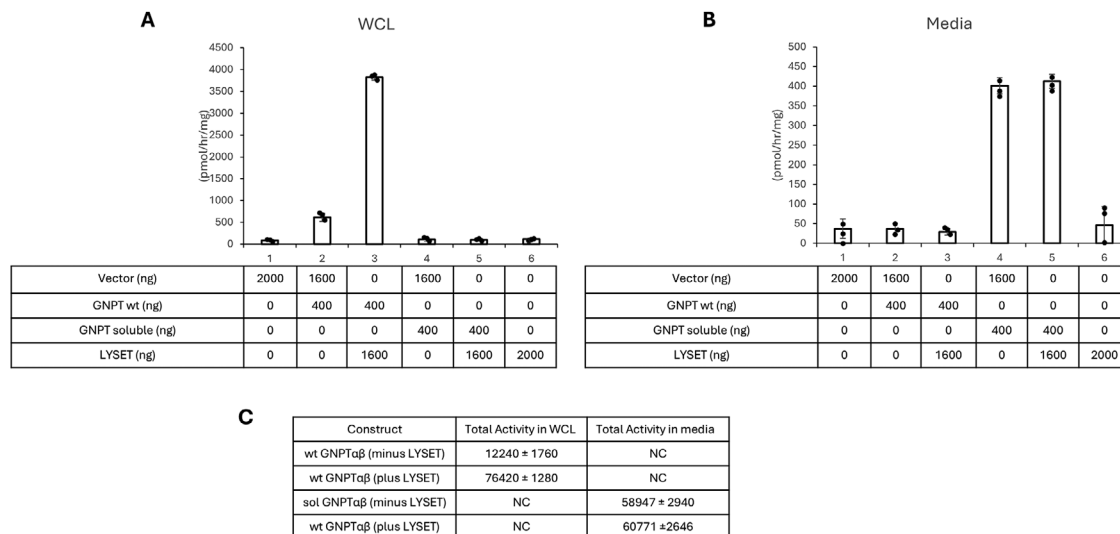
A WCL						
	1	2	3	4	5	6
Vector (ng)	2000	1600	0	1600	0	0
GNPT wt (ng)	0	400	400	0	0	0
GNPT soluble (ng)	0	0	0	400	400	0
LYSET (ng)	0	0	1600	0	1600	2000

B Media						
	1	2	3	4	5	6
Vector (ng)	2000	1600	0	1600	0	0
GNPT wt (ng)	0	400	400	0	0	0
GNPT soluble (ng)	0	0	0	400	400	0
LYSET (ng)	0	0	1600	0	1600	2000

C

Construct	Total Activity in WCL	Total Activity in media
wt GNPTαβ (minus LYSET)	12240 ± 1760	NC
wt GNPTαβ (plus LYSET)	76420 ± 1280	NC
sol GNPTαβ (minus LYSET)	NC	58947 ± 2940
wt GNPTαβ (plus LYSET)	NC	60771 ±2646

FIGURE 2: Soluble GNPT$\alpha\beta$ is not retained intracellularly by overexpression of LYSET. (A) ptase activity of WCLs following transfection of the indicated constructs, or combinations thereof, into *LYSET$^{-/-}$* 293T cells. (B) ptase activities in the cell culture media from A were determined using 15 μl of media following centrifugation at 500×g. (C) Total ptase activity was calculated for WCL (200 μl total) and media (2200 μl) to evaluate the influence of LYSET coexpression on wt GNPT$\alpha\beta$ or soluble GNPT$\alpha\beta$ lacking both TM helices. All activity data are mean ± SD for three independent transfections. NC - not calculated.

than 6-fold increase in the activity of wt GNPT$\alpha\beta$ in the presence of LYSET (Figure 2A, compare lanes 2 and 3), whereas no significant activity beyond background was observed with the soluble GNPT$\alpha\beta$ in the absence or presence of LYSET (Figure 2A, lanes 4 and 5). Instead, all the activity of the soluble GNPT$\alpha\beta$ was detected in the media and LYSET expression had no effect on this secreted activity (Figure 2B, lanes 4 and 5). When the total intracellular activity of the wt GNPT$\alpha\beta$ in WCL was calculated, greater than 80% of the activity was lost in the absence of LYSET (Figure 2C), although we cannot conclude with certainty that the protein level of wt GNPT$\alpha\beta$ in the cell was decreased to the same extent. In contrast, the total activity of the soluble secreted enzyme in the media was unaffected by the absence of LYSET (Figure 2C). While it is unclear whether the lack of both TMHs completely precludes an interaction of GNPT$\alpha\beta$ with LYSET, our results clearly show that the soluble enzyme is not retained in the cell by LYSET but instead escapes the degradative pathway and is secreted to the outside.

A GNPT$\alpha\beta$ variant with either the N- or C-terminal TMH/CD alone is up-regulated by LYSET

Despite lacking both TMHs and CDs, soluble GNPT$\alpha\beta$ is catalytically active (Figure 2, B and C) (Kudo and Canfield, 2006). GNPT$\alpha\beta$-S1S3 (henceforth called S1S3) is a hyperactive truncated form of wt GNPT$\alpha\beta$ that does not undergo proteolytic cleavage (Figure 3A) (Liu *et al.*, 2017; Li *et al.*, 2024). Moreover, S1S3 expressed with either the C-terminal TMH/CD alone (S1S3ΔNTM: type-I TM topology, Figure 3A) or the N-terminal TMH/CD alone (S1S3ΔCTM: type-II TM topology, Figure 3A) exits the ER and is localized to the Golgi-like S1S3 (Figure 3B). This afforded an opportunity to address the behavior of each TMH/CD individually. Due to the hyperactive nature of S1S3, even low-level expression of S1S3 (400 ng of transfected DNA) gave substantial activity (10,472 ± 748 pmol/h/mg) in the absence of LYSET and this activity increased 2.9-fold to 30,134 ± 972 pmol/h/mg when coexpressed with LYSET (Figure 3C, compare lanes 2 and 3). Although the absolute activity values obtained with S1S3 are substantially higher than with wt

GNPT$\alpha\beta$ (Liu *et al.*, 2017), the fold-increase in activity of S1S3 coexpressed with LYSET is significantly lower compared with the value for wt GNPT$\alpha\beta$ (compare Figure 3C, lanes 2 and 3 with Figure 2A, lanes 2 and 3). Because the truncation yielding S1S3 removes over 50% of the GNPT$\alpha\beta$ sequence (Figure 3A), we cannot rule out the possibility that part of the deleted sequence may be involved in LYSET interaction, although our data with soluble GNPT$\alpha\beta$ show it is not sufficient for LYSET-mediated retention. In contrast to S1S3, the activity of S1S3ΔNTM lacking its N-terminal TMH and CD was decreased by 6.7-fold in cells lacking LYSET (Figure 3C, lane 4). Because a COPI Golgi recycling motif resides in the N-terminal CD of GNPT$\alpha\beta$ (Liu *et al.*, 2018) and S1S3ΔNTM lacks the N-terminal CD, it may be the case that a larger fraction of S1S3ΔNTM is exiting the Golgi relative to S1S3. In agreement with this, treatment of the transfected *LYSET$^{-/-}$* cells with 0.1 μM Baf A1 for 16 h to prevent Golgi exit increased the activity of S1S3ΔNTM by 2.8-fold (Figure 3D). Coexpression of S1S3ΔNTM with LYSET also increased this value by 2.8-fold from 1500 ± 54 pmol/h/mg to 4257 ± 109 pmol/h/mg (Figure 3C, compare lanes 4 and 5). These results show that S1S3ΔNTM with only its C-terminal TMH/CD is stimulated by LYSET, but without the N-terminal TMH/CD, the activity of this variant even when coexpressed with LYSET is much lower than that of S1S3 in the absence of LYSET (Figure 3C, compare lanes 2 and 5). S1S3ΔCTM lacking its C-terminal TMH and CD, on the other hand, gave similar activity (8993 ± 210 pmol/h/mg) to S1S3 in the absence of LYSET (Figure 3C, compare 2 and 6). Coexpression with LYSET also increased this activity, but only by 1.7-fold to 14,937 ± 259 pmol/h/mg (Figure 3C, compare 6 and 7). This result suggests that anchoring S1S3 via two TMHs elicits the maximum stimulation by LYSET. In preliminary experiments, we found that the protein level of S1S3, as determined by immunoblot analysis, was hardly changed despite the 2.9-fold increase in activity in the presence of LYSET, raising the interesting question whether LYSET is somehow impacting S1S3 ptase activity directly. This finding warrants further investigation into the role of LYSET in regulating GNPT$\alpha\beta$ ptase activity.
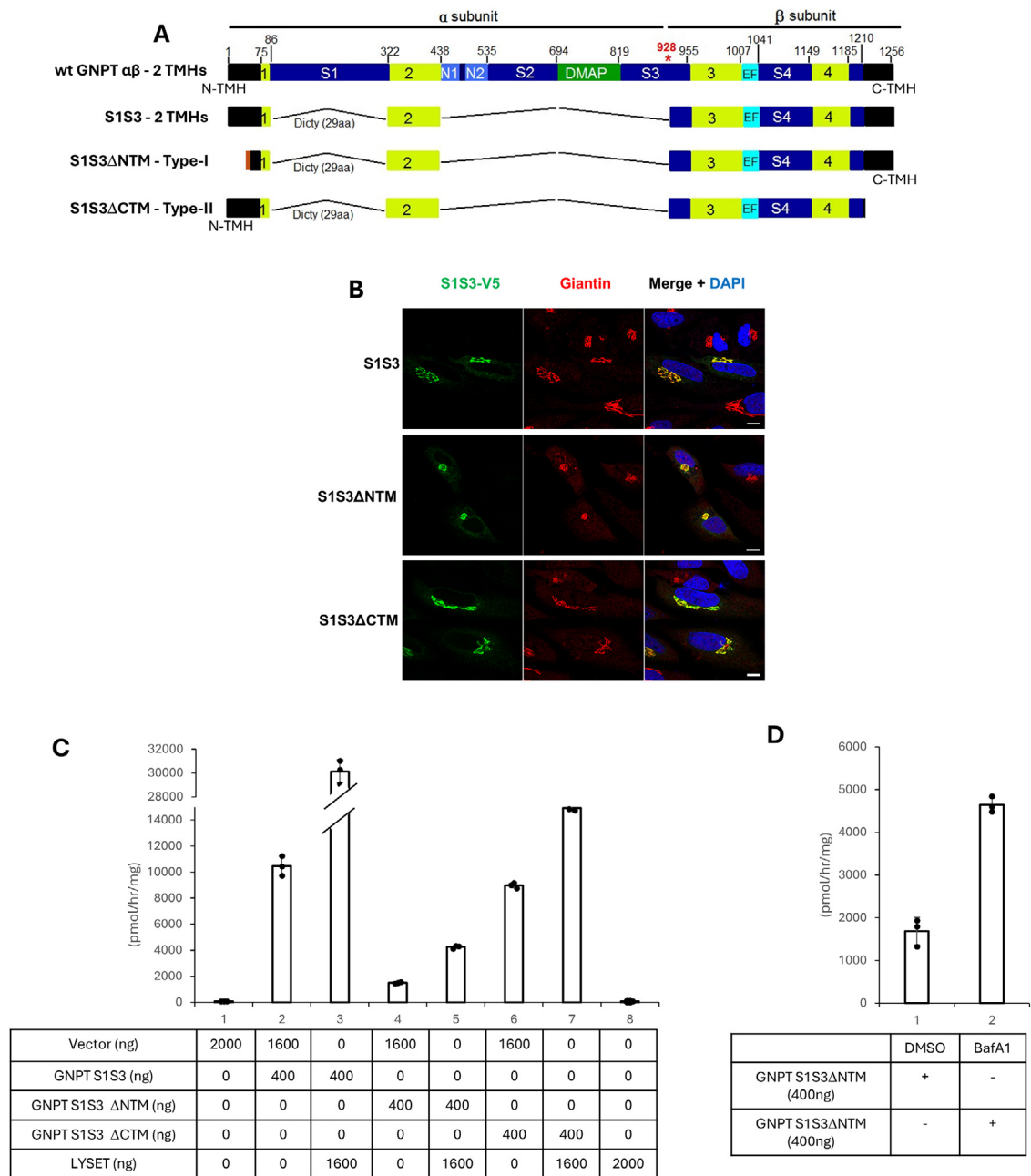
FIGURE 3: LYSET stimulates activity of S1S3 expressed as either type-I or type-II TM protein with a single TMH. (A) Schematic of wt GNPTαβ, S1S3, S1S3ΔNTM, and S1S3ΔCTM. The brown rectangle at the N-terminus of S1S3ΔNTM is the signal peptide of Igκ light chain. The two Notch repeats (N1 and N2), and the DNA methyltransferase-associated protein-interaction (DMAP) domain contribute to recognition of lysosomal hydrolases. The spacer segments (S1–S4) separate the conserved regions (CR) 1–4 (shown in yellow). CR1-4, along with S4 comprise the catalytic core. A calcium-binding EF-hand motif, whose function is not clear, occurs between CR3 and S4. With the exception of the EF-hand and S4, only CR 1-4 are retained in S1S3. The N-terminal TMH spans residues 20–42 while the C-terminal TMH spans residues 1210–1236. (B) Immunofluorescence images of permeabilized HeLa cells transfected with S1S3 (2 TMHs), or S1S3ΔNTM (1 TMH) or S1S3ΔCTM (1 TMH). S1S3 and the variants were probed with an anti-V5 mouse mAb (green) and colocalized with the Golgi marker giantin. Scale bar: 10 μm. (C) Comparison of the ptase activity of S1S3, S1S3ΔNTM, and S1S3ΔCTM expressed alone or in combination with LYSET in *LYSET*⁻/⁻ 293T cells. (D) *LYSET*⁻/⁻ 293T cells transfected to express S1S3ΔNTM were treated 32 h posttransfection with either DMSO or 100 nM BafA1 for 16 h before cells were collected and processed for ptase assay. All activity data are mean ± SD for three independent transfections.
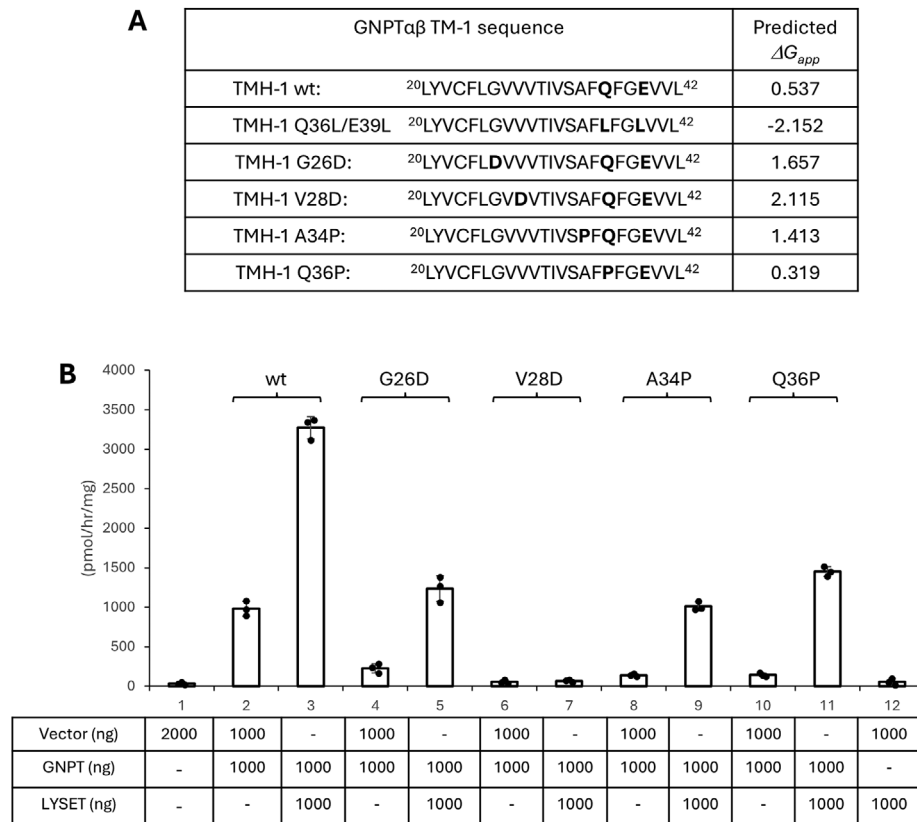
A

	GNPTαβ TM-1 sequence	Predicted ΔG_{app}
TMH-1 wt:	^{20}LYVCFLGVVVTIVSAF**Q**FG**E**VVL^{42}	0.537
TMH-1 Q36L/E39L	^{20}LYVCFLGVVVTIVSAF**L**FG**L**VVL^{42}	-2.152
TMH-1 G26D:	^{20}LYVCFL**D**VVVTIVSAF**Q**FG**E**VVL^{42}	1.657
TMH-1 V28D:	^{20}LYVCFLGV**D**VTIVSAF**Q**FG**E**VVL^{42}	2.115
TMH-1 A34P:	^{20}LYVCFLGVVVTIVS**P**F**Q**FG**E**VVL^{42}	1.413
TMH-1 Q36P:	^{20}LYVCFLGVVVTIVSAF**P**FG**E**VVL^{42}	0.319

B

	1	2	3	4	5	6	7	8	9	10	11	12
Vector (ng)	2000	1000	-	1000	-	1000	-	1000	-	1000	-	1000
GNPT (ng)	-	1000	1000	1000	1000	1000	1000	1000	1000	1000	1000	-
LYSET (ng)	-	-	1000	-	1000	-	1000	-	1000	-	1000	1000

FIGURE 4: Disease-causing mutations in the N-terminal TMH (TMH-1) of GNPTαβ further destabilize the helix causing more of the mutant proteins to exit the Golgi in the absence of LYSET and go to the lysosome for degradation. (A) Prediction of the apparent free energy (ΔG_{app}) for membrane insertion for wt GNPTαβ and the various N-terminal TM helix mutations using the ΔG prediction server v1.0. (B) Comparison of the ptase activity of wt GNPTαβ and the various N-terminal TM helix mutations expressed alone or in combination with LYSET in LYSET$^{-/-}$ 293T cells. The activity data are the mean ± SD for three independent transfections.

Patient mutations in the N-terminal TMH of GNPTαβ further destabilize the helix

We previously analyzed several disease-causing mutations in the N-terminal TMH of GNPTαβ (Velho *et al.*, 2019; Wang *et al.*, 2019) and found that they either caused GNPTαβ to exit the Golgi and go to the lysosome for degradation (G26D, A34P, and Q36P), or prevented it from translocating from the cytoplasm into the lumen of the ER (V28D) (Lee *et al.*, 2020). A prediction of the apparent free energy (ΔG_{app}) for membrane insertion of wt and mutant TMHs is shown in Figure 4A. As reported previously (Pechincha *et al.*, 2022), the Q36L/E39L double mutation changed the ΔG_{app} value from 0.537 to −2.152, which explains the increased stability of this mutant since a negative ΔG favors membrane insertion (Babakhani *et al.*, 2008). All the patient mutations (with exception of Q36P), on the other hand, increased the hydrophilicity of the TMH relative to wt, with V28D showing the most positive ΔG_{app} value. In the case of Q36P, it is more likely that a proline residue at this position results in a break in the α-helix, especially since the proline is located close to the C-terminal end of the TMH (Nilsson *et al.*, 1998). This analysis suggests that the patient mutations within TMH-1 of GNPTαβ further destabilize the helix such that the mutant proteins either leave the Golgi or fail to get into the ER. The activity of these mutant proteins, relative to wt, in *LYSET$^{-/-}$* 293T cells under conditions of moderate expression (1 μg of transfected DNA) ranged from 23% (G26D) to near vector-only value (V28D) (Figure 4B, compare lane 2 with lanes 4, 6, 8, and 10). Except for V28D, coexpression of LYSET increased the activity of the mutant proteins from 31 to 44% of wt (Figure 4B, compare lane 3 with lanes 5, 9, and 11), showing that overexpressed LYSET can partially rescue the effect of the mutations. Because the V28D mutant cannot translocate into the lumen of the ER (Lee *et al.*, 2020), it is not surprising that that LYSET did not exert a positive effect on this mutant (Figure 4B, compare lanes 6 and 7).

Recycling via COPI binding is still critical for Golgi retention of GNPTαβ despite membrane stabilization

Because the membrane-stabilized variant of GNPTαβ (Q36L/E39L) displayed good activity in cells lacking LYSET, it begged the question as to how important vesicular recycling is in this context for the steady-state Golgi localization and activity of the variant. To address this, the N-terminal CD patient mutation (K4Q) which abrogates interaction with COPI coatomer (Liu *et al.*, 2018) was introduced into GNPTαβ Q36L/E39L to generate a triple mutant. In the absence of LYSET, under conditions of moderate expression (1 μg of transfected DNA), the triple mutant showed only 5% of activity relative to GNPTαβ Q36L/E39L (Figure 5, compare lanes 2 and 4). While coexpression with LYSET increased the activity of the triple mutant 6.3-fold (Figure 5, compare lanes 4 and 5), this activity was still substantially lower than that of GNPTαβ Q36L/E39L in the absence of LYSET (Figure 5, compare lanes 2 and 5). These results suggest that despite being stably integrated into the Golgi membrane, GNPTαβ Q36L/E39L upon reaching the TGN must still bind

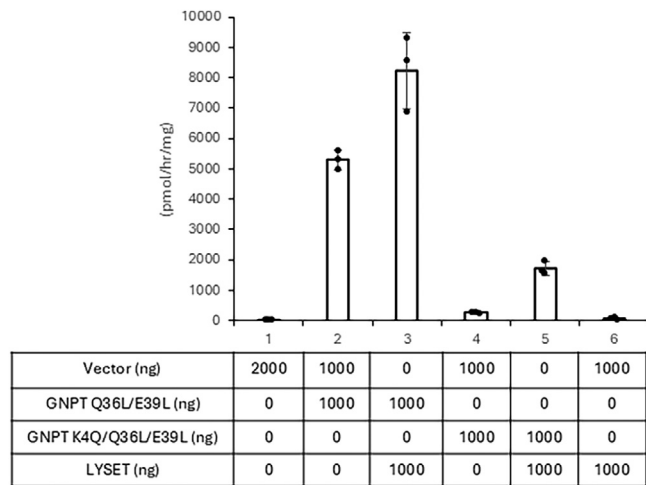|	1	2	3	4	5	6
Vector (ng)	2000	1000	0	1000	0	1000
GNPT Q36L/E39L (ng)	0	1000	1000	0	0	0
GNPT K4Q/Q36L/E39L (ng)	0	0	0	1000	1000	0
LYSET (ng)	0	0	1000	0	1000	1000

FIGURE 5: The K4Q substitution in GNPT$\alpha\beta$ Q36L/E39L negates the positive effect of the membrane-stabilizing amino acid changes. Comparison of the ptase activity of GNPT$\alpha\beta$ Q36L/E39L and GNPT$\alpha\beta$ K4Q/Q36L/E39L expressed alone or in combination with LYSET in $LYSET^{-/-}$ 293T cells. The activity data are the mean $\pm$ SD for three independent transfections.

COPI and be recycled to achieve steady-state Golgi localization. In the absence of COPI binding, membrane stabilization or LYSET-mediated Golgi-tethering alone is insufficient to keep GNPT$\alpha\beta$ in the Golgi, which helps explain why patients with the K4Q mutation acquire disease even though LYSET is present (Leroy *et al.*, 2014).

Closing thoughts
Our study provides evidence that both TMHs/CDs of GNPT$\alpha\beta$ contribute to LYSET-mediated membrane stabilization to prevent the exit of GNPT$\alpha\beta$ from the Golgi and its degradation in the lysosome. The finding that S1S3 with both TMHs/CDs is stimulated to a greater degree by LYSET than the two variants with a single TMH/CD, together with our previous work showing that LYSET adopts a two TMH topology with both N- and C-terminal CDs in the cytoplasm, presents an interesting scenario whereby one TMH of GNPT$\alpha\beta$ is stabilized by the other TMH of LYSET, and vice versa. Finally, our results emphasize the cooperative nature of LYSET and COPI binding to GNPT$\alpha\beta$ in helping retain the latter in the Golgi.

MATERIALS AND METHODS
Request a protocol through *Bio-protocol*

Reagents and antibodies
UDP-[^{3}H]GlcNAc (20–45 Ci/mmol) was purchased from Revvity LifeScience (Waltham, MA, USA). Mouse anti-V5 mAb (Catalogue no. 46-0705) was obtained from Thermo Fisher Scientific (Waltham, MA, USA) while anti-giantin rabbit polyclonal antibody (Catalogue no. 924302) was from BioLegend (San Diego, CA, USA). Anti-Flag-M2 agarose beads and methyl α-D-mannopyranoside (α-MM) were both purchased from Millipore-Sigma (St. Louis, MO, USA).

DNA constructs
The generation of the plasmids GNPT$\alpha\beta$-V5-pcDNA6 (including the G26D, V28D, A34P, and Q36P mutants), S1S3-V5-pcDNA6, LYSETpCDNA3.1, and LYSET-3XFlag-pcDNA3.1 has been described (van Meel *et al.*, 2014; Liu *et al.*, 2017; Lee *et al.*, 2020; Zhang *et al.*, 2022). The plasmids with mutations in the N-

terminal TMH (GNPT$\alpha\beta$ Q36L/E39L-V5-pcDNA3.1 and GNPT$\alpha\beta$ K4Q/Q36L/E39L-V5pcDNA3.1) were generated by a two-step overlap-extension PCR wherein the wt DNA fragment encoding the first 364 aa of GNPT$\alpha\beta$ was swapped for the same size fragment harboring the individual mutation/s by restriction digest and ligation. The plasmid encoding soluble GNPT$\alpha\beta$ lacking both TMHs was synthesized at GenScript (Piscataway, NJ, USA). In this construct in the vector pcDNA3.1, nucleotides encoding the Igκ light chain signal peptide sequence were included at the 5′ end of the GNPT$\alpha\beta$ cDNA which started at the codon for amino acid 44. In addition, the nucleotides encoding the S1P cleavage site within the cDNA were switched to encode for a furin cleavage site for efficient processing (Kudo and Canfield, 2006). S1S3∆NTM-V5pcDNA3.1 and S1S3∆CTM-V5pcDNA3.1 were also synthesized at Genscript. S1S3∆NTM includes the Igκ light chain signal peptide sequence at the 5′ end of the cDNA. DNA sequencing was performed to verify that all constructs were correct.

Mammalian cell culture and cell engineering
HEK293T and HeLa cells were acquired from ATCC (Manassas, VA, USA) and maintained in DMEM containing 0.11 g/l sodium pyruvate and 4.5 g/l glucose, supplemented with 10% (vol/vol) FBS, 100,000 U/l penicillin, 100 mg/l streptomycin and 2 mM L-glutamine. Cells were cultured at 37°C in the presence of 5% CO$_2$ humidified incubator.

LYSET 293T knockout cells were generated as described by Ran *et al.* (Ran *et al.*, 2013). Briefly, the single-guideRNA (sgRNA) (5′ – TGTCCACACCCAAAAAGGCA – 3′) was ligated into pspCas9 (BB)-2A-Puro (Addgene, 48139) plasmid. Cells were transfected with the CRISPR-Cas9 knockout plasmid using Lipofectamine 2000 (Thermo Fisher Scientific) according to the manufacturer's instruction. A total of 24 h posttransfection, cells were treated with 1 µg/ml puromycin (Invitrogen) for 2–3 d. For single colony isolation, cells were then diluted into 96-well plates to a final concentration of 0.5 cell per well. The colonies were further screened by Western blot analysis, and the candidate clean knockout colonies were verified by sequencing analysis to confirm the indels at their target sites. All cell cultures tested negative for *Mycoplasma* contamination with the Mycoalert mycoplasma detection kit (Lonza).

Transient transfection
Cells were plated to ~50% confluency and transfected with either individual plasmids or cotransfected with the two indicated plasmids (total of 2 µg DNA per well in a 6-well plate) using jetOPTIMUS transfection reagent from Polyplus (Sartorius, Illkirch, France) according to the manufacturer's protocol. Cells in 6-well plates were harvested 48 h posttransfection and lysed in 200 µl of buffer A (25 mM Tris-Cl, pH 7.2, 150 mM NaCl, 1% Triton-X 100 and protease inhibitor cocktail).

ptase activity assays
The protocol for measuring GlcNAc-ptase activity (calculated from the amount of [^{3}H]GlcNAc-1P that is transferred from the radio-labeled nucleotide sugar donor UDP-GlcNAc to the synthetic acceptor α-MM) was adapted from van Meel *et al.* (van Meel *et al.*, 2016), with some modifications. WCLs (50 µg) prepared in buffer A were assayed in a final volume of 50 µl in buffer containing 50 mM Tris (pH 7.4), 10 mM MgCl$_2$, 10 mM MnCl$_2$, 2 mg/ml BSA, 2 mM ATP, 75 µM UDP-GlcNAc, and 1 µCi UDP-[^{3}H]GlcNAc, with 100 mM α-MM as acceptor. The reactions were performed at 37°C for 1 h, quenched with 950 µl of 5 mM EDTA (pH 8.0), and the samples applied to a QAE-Sephadex column (1 ml of packed beads

equilibrated with 2 mM Tris, pH 8.0). The columns were washed twice, first with 3 ml of 2 mM Tris (pH 8.0), then with 2 ml of the same buffer. Elution was performed twice directly into liquid scintillation vials, first with 3 ml of 2 mM Tris (pH 8.0) containing 30 mM NaCl, then once again with 2 ml of the same buffer. A total of 8 ml of EcoLite scintillation fluid (MP Biomedicals) was then added to the vials, and the radioactivity in the collected fractions was measured using a Beckman LS6500 scintillation counter. All counts per minute (CPM) values that were obtained after subtracting buffer-only background were converted to pmol of GlcNAc-1P transferred to α-MM per hour per mg total protein lysate (pmol/h/mg).

Immunofluorescence microscopy

To visualize the subcellular localization of the S1S3, S1S3ΔNTM and S1S3ΔCTM, HeLa cells were transfected with the various cDNA using the jetOPTIMUS transfection reagent. The cells were fixed 24–36 h posttransfection with 4% formaldehyde (Sigma-Aldrich) for 10 min, permeabilized and blocked with PBS containing 0.4% (vol/vol) Triton X-100 and 2% IgG free BSA (Jackson ImmunoResearch) for 1 h, and then probed with the indicated combinations of antibodies in PBS containing 0.1% Triton X-100 and 0.5% BSA. The processed cells were mounted in ProLong Gold antifade mounting medium (Life Technologies), and the images were acquired with an LSM880 confocal microscope (Carl Zeiss Inc., Peabody, MA). Images were analyzed by Image J software (Fiji).

ΔG_{app} prediction

For prediction of the apparent free energy (ΔG_{app}) for membrane insertion of the wt and mutant TMHs of GNPT$\alpha\beta$, the ΔG predictor (https://dgpred.cbr.su.se/index.php?p=TMpred) was utilized (Hessa et al., 2007).

REFERENCES

Ain NU, Muhammad N, Dianatpour M, Baroncelli M, Iqbal M, Fard MAF, Bukhari I, Ahmed S, Hajipour M, Tabatabaie Z, et al. (2021). Biallelic TMEM251 variants in patients with severe skeletal dysplasia and extreme short stature. Hum Mutat 42, 89–101.

Babakhani A, Gorfe AA, Kim JE, McCammon JA (2008). Thermodynamics of peptide insertion and aggregation in a lipid bilayer. J Phys Chem B 112, 10528–10534.

Braulke T, Carette JE, Palm W (2024). Lysosomal enzyme trafficking: From molecular mechanisms to human diseases. Trends Cell Biol 34, 198–210.

Ghosh P, Dahms NM, Kornfeld S (2003). Mannose 6-phosphate receptors: New twists in the tale. Nat Rev Mol Cell Biol 4, 202–212.

Hessa T, Meindl-Beinker NM, Bernsel A, Kim H, Sato Y, Lerch-Bader M, Nilsson I, White SH, von Heijne G (2007). Molecular code for transmembrane-helix recognition by the Sec61 translocon. Nature 450, 1026–1030.

Kollmann K, Pohl S, Marschner K, Encarnacao M, Sakwa I, Tiede S, Poorthuis BJ, Lubke T, Muller-Loennies S, Storch S, et al. (2010). Mannose phosphorylation in health and disease. Eur J Cell Biol 89, 117–123.

Kornfeld S (1986). Trafficking of lysosomal enzymes in normal and disease states. J Clin Invest 77, 1–6.

Kudo M, Bao M, D'Souza A, Ying F, Pan H, Roe BA, Canfield WM (2005). The alpha- and beta-subunits of the human UDP-N-acetylglucosamine:lysosomal enzyme N-acetylglucosamine-1-phosphotransferase [corrected] are encoded by a single cDNA. J Biol Chem 280, 36141–36149.

Kudo M, Brem MS, Canfield WM (2006). Mucolipidosis II (I-cell disease) and mucolipidosis IIIA (classical pseudo-hurler polydystrophy) are caused by mutations in the GlcNAc-phosphotransferase alpha /beta -subunits precursor gene. Am J Hum Genet 78, 451–463.

Kudo M, Canfield WM (2006). Structural requirements for efficient processing and activation of recombinant human UDP-N-acetylglucosamine:lysosomal-enzyme-N-acetylglucosamine-1-phosphotransferase. J Biol Chem 281, 11761–11768.

Lee WS, Jennings BC, Doray B, Kornfeld S (2020). Disease-causing missense mutations within the N-terminal transmembrane domain of GlcNAc-1-phosphotransferase impair endoplasmic reticulum translocation or Golgi retention. Hum Mutat 41, 1321–1328.

Leroy JG, Sillence D, Wood T, Barnes J, Lebel RR, Friez MJ, Stevenson RE, Steet R, Cathey SS (2014). A novel intermediate mucolipidosis II/IIIalphabeta caused by GNPTAB mutation in the cytosolic N-terminal domain. Eur J Hum Genet 22, 594–601.

Li H, Doray B, Jennings BC, Lee WS, Liu L, Kornfeld S, Li H (2024). Structure of a truncated human GlcNAc-1-phosphotransferase variant reveals the basis for its hyperactivity. J Biol Chem 300, 107706.

Liu L, Doray B, Kornfeld S (2018). Recycling of Golgi glycosyltransferases requires direct binding to coatomer. Proc Natl Acad Sci U S A 115, 8984–8989.

Liu L, Lee WS, Doray B, Kornfeld S (2017). Engineering of GlcNAc-1-phosphotransferase for production of highly phosphorylated lysosomal enzymes for enzyme replacement therapy. Mol Ther Methods Clin Dev 5, 59–65.

Marschner K, Kollmann K, Schweizer M, Braulke T, Pohl S (2011). A key enzyme in the biogenesis of lysosomes is a protease that regulates cholesterol metabolism. Science 333, 87–90.

Nilsson I, Saaf A, Whitley P, Gafvelin G, Waller C, von Heijne G (1998). Proline-induced disruption of a transmembrane alpha-helix in its natural environment. J Mol Biol 284, 1165–1175.

Paik KH, Song SM, Ki CS, Yu HW, Kim JS, Min KH, Chang SH, Yoo EJ, Lee IJ, Kwan EK, et al. (2005). Identification of mutations in the GNPTA (MGC4170) gene coding for GlcNAc-phosphotransferase alpha/beta subunits in Korean patients with mucolipidosis type II or type IIIA. Hum Mutat 26, 308–314.

Pechincha C, Groessl S, Kalis R, de Almeida M, Zanotti A, Wittmann M, Schneider M, de Campos RP, Rieser S, Brandstetter M, et al. (2022). Lysosomal enzyme trafficking factor LYSET enables nutritional usage of extracellular proteins. Science 378, eabn5637.

Ran FA, Hsu PD, Wright J, Agarwala V, Scott DA, Zhang F (2013). Genome engineering using the CRISPR-Cas9 system. Nat Protoc 8, 2281–2308.

Richards CM, Jabs S, Qiao W, Varanese LD, Schweizer M, Mosen PR, Riley NM, Klussendorf M, Zengel JR, Flynn RA, et al. (2022). The human disease gene LYSET is essential for lysosomal enzyme transport and viral infection. Science 378, eabn5648.

Tawfeek HA, Abou-Samra AB (2004). Important role for the V-type H(+)-ATPase and the Golgi apparatus in the recycling of PTH/PTHrP receptor. Am J Physiol Endocrinol Metab 286, E704–E710.

Tiede S, Storch S, Lubke T, Henrissat B, Bargal R, Raas-Rothschild A, Braulke T (2005). Mucolipidosis II is caused by mutations in GNPTA encoding the alpha/beta GlcNAc-1-phosphotransferase. Nat Med 11, 1109–1112.

van Meel E, Lee WS, Liu L, Qian Y, Doray B, Kornfeld S (2016). Multiple domains of GlcNAc-1-phosphotransferase mediate recognition of lysosomal enzymes. J Biol Chem 291, 8295–8307.

van Meel E, Qian Y, Kornfeld SA (2014). Mislocalization of phosphotransferase as a cause of mucolipidosis III alphabeta. Proc Natl Acad Sci U S A 111, 3532–3537.

Velho RV, Harms FL, Danyukova T, Ludwig NF, Friez MJ, Cathey SS, Filocamo M, Tappino B, Gunes N, Tuysuz B, et al. (2019). The lysosomal storage disorders mucolipidosis type II, type III alpha/beta, and type III gamma: Update on GNPTAB and GNPTG mutations. Hum Mutat 40, 842–864.

Wang Y, Ye J, Qiu WJ, Han LS, Gao XL, Liang LL, Gu XF, Zhang HW (2019). Identification of predominant GNPTAB gene mutations in Eastern Chinese patients with mucolipidosis II/III and a prenatal diagnosis of mucolipidosis II. Acta Pharmacol Sin 40, 279–287.

Yang X, Doray B, Venkatarangan V, Jennings BC, Henn D, Liang J, Zhao H, Zhang W, Zhang B, Yu L, et al. (2024). Molecular insights into the regulation of GNPTAB by TMEM251. bioRxiv.

Zhang W, Yang X, Li Y, Yu L, Zhang B, Zhang J, Cho WJ, Venkatarangan V, Chen L, Burugula BB, et al. (2022). GCAF(TMEM251) regulates lysosome biogenesis by activating the mannose-6-phosphate pathway. Nat Commun 13, 5351.